ORAL SCI HOMEOST MED

Open Access
ORIGINAL ARTICLE

SPECIAL ISSUE: Oral Regional Immune Mechanisms and Systemic Homeostasis

A simplified 3D oral epithelial model using an air-liquid interface culture system

Liu Liu[1], Jiang Liu[1], Yao Yuan[1] ✉, and Hang Zhao[1] ✉

[1] *State Key Laboratory of Oral Diseases & National Center for Stomatology & National Clinical Research Center for Oral Diseases & Research Unit of Oral Carcinogenesis and Management & Chinese Academy of Medical Sciences, West China Hospital of Stomatology, Sichuan University, Chengdu, 610041, China*

Cite This: *Oral Sci Homeost Med*, 2026, 2, 9610045

Read Online

ABSTRACT: Three-dimensional (3D) epithelial models are widely used to investigate epithelial biology, host-pathogen interactions, and topical therapeutics. However, many existing models rely on primary keratinocytes or specific cell lines, limiting accessibility, reproducibility, and scalability. Besides, reliable oral epithelial models based on stable keratinocyte cell lines remain limited, as most current systems depend on primary cells or organotypic cultures. In this study, we established simplified and reproducible 3D epithelial models using an optimized air-liquid interface (ALI) culture system with two human keratinocyte cell lines, HaCaT (epidermal) and HOK (oral). After culture condition optimization, both cell types maintained stable stratification and differentiation across multiple passages. Histological analysis showed well-organized epithelial architectures with distinct basal and suprabasal layers. Immunofluorescence staining confirmed spatially distinct expression of epithelial differentiation markers closely resembling native epithelia. Functionally, the reconstructed epithelia robust barrier integrity and responded to *Candida albicans* infection. Moreover, the models allowed evaluation of drug permeability across epithelial layers. Collectively, this simplified 3D culture platform provides a reproducible, accessible strategy for constructing epithelial models using standardized keratinocyte cell lines without primary cells. The system offers a practical tool for oral and cutaneous epithelial research, with potential in infection studies, disease modeling, and preclinical drug screening.

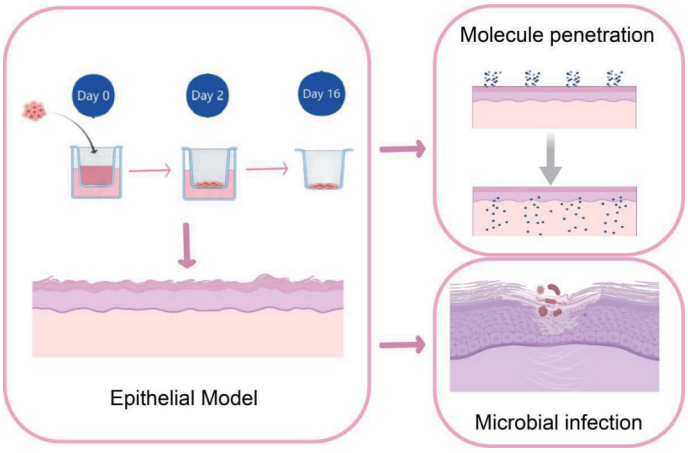

KEYWORDS: 3D culture model, keratinocytes, differentiation, oral mucosa, drug permeability, host-pathogen interaction

1 Introduction

As a stratified squamous epithelium covering the oral mucosa and skin surfaces, epithelial tissue serves as a critical barrier that protects the body from environmental insults while maintaining tissue homeostasis. Beyond its structural role, the epithelium actively participates in immune regulation and host pathogen interactions, making it essential in the pathogenesis of numerous inflammatory and infectious diseases. Consequently, epithelial biology represents a central focus in dermatological, dental, and oral biomedical research[1-3]. Currently, investigations of epithelial biology have relied heavily on clinical specimens and animal models. Clinical samples provide valuable physiological insights but are often constrained by donor heterogeneity, limited availability, and ethical considerations. Animal models offer controlled experimental systems; however, they frequently fail to accurately reproduce human specific epithelial characteristics, including differences in stratum corneum structure, immune responsiveness, and the composition of commensal microbiota[4]. Two-dimensional (2D) cell culture systems have therefore been widely adopted as an alternative experimental platform. While these models offer simplicity and experimental convenience, they lack the three-dimensional (3D) architecture and microenvironment required to maintain epithelial polarity, stratified differentiation, and physiological interactions[5]. As a consequence, 2D systems provide limited capacity to accurately model epithelial barrier function, drug permeability, and pathogen host interactions[6].

To overcome these limitations, significant efforts have been directed toward developing three-dimensional epithelial models that better recapitulate the structural and functional characteristics

Received: February 5, 2026; **Revised:** March 13, 2026
Accepted: March 29, 2026

✉Address correspondence to Yao Yuan, yaoyuan_sklo@scu.edu.cn; Hang Zhao, zhaohangahy@scu.edu.cn

of native tissues[7]. Several reconstructed epithelial systems are capable of forming stratified layers and some have even been translated into commercial products. Nevertheless, important challenges remain. Many current models rely heavily on primary epithelial cells, which introduces issues such as donor variability, limited expansion capacity, and repeated ethical approval requirements[8]. Other systems require technically demanding culture procedures or specialized cell sources[9], leading to reduced reproducibility and poor inter laboratory standardization[10]. In addition, the high cost associated with these systems restricts their accessibility in long-term studies and large scale applications. Notably, standardized oral epithelial models based on stable keratinocyte cell lines remain limited, which further constrains *in vitro* research in oral biology and disease studies.

To address these challenges, we aimed to develop a simplified, accessible, and reproducible 3D in vitro epithelial model using keratinocyte cell lines widely utilized in dermatological and oral research. In this study, human derived keratinocyte lines were combined with an optimized air-liquid interface (ALI) culture protocol to generate stratified epithelia capable of sustained proliferation and differentiation in a 3D environment. The resulting model was comprehensively characterized for its morphological and functional fidelity and further evaluated for its ability to mimic pathological microenvironments and assess drug permeability. This platform provides a practical and scalable strategy for epithelial biology research, disease modeling, and therapeutic development.

2 Materials and methods

2.1 Cell culture

Human-derived skin keratinocytes HaCaT and oral-derived keratinocytes HOK and NOK were provided by the State Key Laboratory of Oral Disease Research, Sichuan University. Human keratinocyte cell lines (HaCaT and HOK) were cultured using a keratinocyte medium (KeraPrime™, K0802, ES MedTech Inc.), specifically optimized for epithelial proliferation and stratification. Three-dimensional epidermal models were constructed based on an ALI system optimized according to the 3D culture platform (EpiPrime™, E0602, ES MedTech Inc.). The product was purchased for experimental use and applied according to the manufacturer's instructions. Histological and functional validation of the model is described in detail below. All experiments were performed in accordance with standardized operating procedures to ensure reproducibility.

In this study, a modular culture system with staged regulation was designed based on four functionally complementary medium components, named BM-1, BM-2, BM-3 and BM-4 (ES MedTech Inc.), respectively. In the two-dimensional monolayer culture stage, HOK require no modification to existing culture protocols, while BM-1/BM-2 mixed medium (9:1 v/v) was used for HaCaT separated culture, which can meet the regular cell proliferation requirements. When transferred to the 3D insert culture system with 0.4 μm pore size (NEST, China), 1.5×10^5 cells were spread into the upper layer of Insert with a volume of 200 μL, and a phased medium conditioning strategy was implemented: the initial 48 hours, HOK and HaCaT were both in BM-1, and 1 mL of it was added to the lower layer of Insert to achieve cell proliferation balanced with stemness maintenance. From the third day onwards, the medium of HaCaT was changed to differentiation-inducing medium BM-1/BM-3 (499:1 v/v), while medium of HOK was changed to differentiation-inducing medium BM-4, and 0.5 mL was added to the lower layer of Insert, and the upper layer of liquid was removed to form an air-liquid interface to induce directional differentiation. The whole differentiation cycle lasted for 14 days, during which the lower layer of medium was changed every 24 hours and the upper layer of exudate liquid was aspirated. The culture conditions were constant at 37°C and 5% CO_2. The final cell phenotype was verified by fixation, dehydration, embedding, sectioning, and staining[11].

2.2 Hematoxylin & Eosin (H&E) staining

Sections of keratinocyte cultures were placed in an oven at a constant temperature of 65°C and baked for 2 h. The sections were then subjected to sequential deparaffinization and hydration: deparaffinization in xylene I and II for 15 min each, followed by hydration in graded alcohol (100% I for 5 min, 100% II for 5 min, 95% for 5 min, 80% for 2 min, and 75% for 2 min). After hydration, the sections were washed three times with distilled water for 5 min each, stained with hematoxylin for 30 s, rinsed in running tap water for 15 min, and counterstained with 0.5% eosin for 30 s to 1 min. Finally, the samples were allowed to air-dry, mounted, and observed using a whole-slide tissue scanner (Olympus VS200, Japan).

2.3 Immunofluorescence (IF)

Sections of keratinocyte cultures were placed in a 65°C constant-temperature oven and baked for 2 h. The sections were subjected to sequential deparaffinization and hydration: deparaffinized in xylene I and II for 15 min each, then hydrated in graded alcohol (100% I for 5 min, 100% II for 5 min, 95% for 5 min, 80% for 2 min, 75% for 2 min). After washing three times with distilled water for 5 min each, the sections were blocked with 5% bovine serum albumin (BSA) at room temperature for 1 h, then incubated overnight at 4°C with primary antibodies.The next day, the samples were washed three times with distilled water for 5 min each, incubated with fluorescently labeled secondary antibodies at room temperature for 1 h in the dark, and washed three times with distilled water for 5 min each. The sections were then stained with 4',6-diamidino-2-phenylindole (DAPI) solution (Servicebio, China) for 5 min, followed by another three washes with distilled water for 5 min each. Finally, the samples were air-dried, mounted, and observed using a whole-slide tissue scanner (Olympus VS200, Japan).

2.4 Immunohistochemistry (IHC)

Sections of keratinocyte cultures were placed in a constant-temperature oven at 65°C and baked for 2 h. The sections were sequentially subjected to deparaffinization and hydration: deparaffinized in xylene I and II for 15 min each, then hydrated in graded alcohol (100% I for 5 min, 100% II for 5 min, 95% for 5 min, 80% for 2 min, 75% for 2 min), and washed three times with distilled water for 5 min each. The sections were immersed in citrate antigen retrieval solution (Beyotime, China), heated in an autoclave for 5 min for antigen retrieval, and cooled to room temperature. After cooling, the sections were washed three times with distilled water for 5 min each. Endogenous peroxidase activity was blocked with an appropriate volume of endogenous peroxidase blocker at room temperature for 10 min. The sections were then washed three times with distilled water for 5 min each and blocked with goat serum (ZSGB-BIO, China) for 1 h. An appropriate

volume of primary antibody was added dropwise according to tissue size, and the sections were incubated at 4°C overnight. The next day, the sections were washed three times with distilled water for 5 min each. An appropriate volume of reaction enhancer was added dropwise, and the sections were incubated for 20 min, followed by three washes with distilled water for 5 min each. Horseradish peroxidase-labeled goat anti-mouse/rabbit IgG polymer was then added dropwise and incubated for 1 h, and the sections were washed three times with distilled water for 5 min each. DAB staining solution was added dropwise, and color development was monitored under a microscope. The reaction was stopped at an appropriate time. The sections were counterstained with hematoxylin for 30 s, rinsed in distilled water two or more times for 3 s each until excess dye was removed, and then rinsed in running tap water for 15 min. The samples were air-dried, mounted, and observed using a whole-slide tissue scanner (Olympus VS200, Japan).

2.5 Antibodies

For IF, Keratin 5(#905504), Keratin 6(#606102), Keratin 10(#905404), Keratin 18(#628402) were purchased from BioLegend. The antibody for E-Cadherin(#20874-1-AP) was purchased from Proteintech. For IHC, Anti-Ki67(#ab16667) was purchased from abcam.

2.6 Fluorescein isothiocyanate (FITC) transdermal permeation assay

FITC (1 mg/mL) was prepared in DMSO, diluted to 10 μg/mL with distilled water, applied to the cultures, and incubated for 12, 24, and 48 h. The samples were then stained with DAPI in the dark for 5 min and washed three times with distilled water for 5 min each. Finally, the samples were air-dried, mounted, and observed using a whole-slide tissue scanner (Olympus VS200, Japan).

The depth of FITC penetration and the total thickness of the tissue model were measured using ImageJ. Penetration depth was defined as the perpendicular distance from the apical surface to the leading edge of FITC fluorescence. The penetration rate was calculated as the ratio of the penetration depth to the total thickness of the tissue model and expressed as a percentage.

Permeability was measured over time using three independent biological replicates. Data are presented as the mean ± standard deviation (SD) at each time point to illustrate the trend and variability of the permeation profile.

2.7 3D model of *Candida albicans (C. albicans)* infection

10 mL of *C. albicans* cultured in broth supplemented with 0.5% (w/v) dextrose was incubated at 37°C overnight. Yeast cells were harvested by centrifugation at 3000 rpm for 5 min, and the pellet was washed three times with 6 mL of sterile PBS, then resuspended in yeast extract peptone dextrose (YPD) medium to adjust the concentration to 1×10^7 colony-forming units/mL (CFU/mL) [12]. On day 12 of 3D culture, the models were inoculated with a *Candida* suspension containing 2×10^6 CFU and incubated at 37°C for 12, 24, and 48 h.

2.8 Periodic Acid-Schiff (PAS) staining

Sections of keratinocyte cultures were placed in a constant-temperature oven at 65°C and baked for 2 h. The sections were then subjected to sequential deparaffinization and hydration: deparaffinized in xylene I and II for 15 min each, hydrated in graded alcohol (100% I for 5 min, 100% II for 5 min, 95% for 5 min, 80% for 2 min, 75% for 2 min), and washed three times with distilled water for 5 min each.PAS staining was performed using a commercial kit (Beyotime, China). Periodic acid solution was equilibrated to room temperature, and 100 μL was added dropwise to each sample. Samples were incubated in a humidified chamber in the dark for 10 min. After removing the periodic acid solution, the sections were immersed in distilled water and washed on a shaker for 5 min. 100 μL of Schiff's reagent was added dropwise to each sample, and the sections were incubated in a humidified chamber at 37°C in the dark.After removing the staining solution, the sections were soaked in distilled water and washed on a shaker for 5 min. Each sample was counterstained with 100 μL hematoxylin solution for 30 s. The staining solution was removed, and the sections were rinsed two or more times in distilled water for 3 s each until excess dye was removed, followed by rinsing in running tap water for 15 min.The samples were air-dried, mounted, and observed using a whole-slide tissue scanner (Olympus VS200, Japan).

3 Results

3.1 Establishment of a stratified 3D human epidermal model using HaCaT cells

To establish a three-dimensional epidermal model, HaCaT keratinocytes were cultured under optimized ALI conditions. During the initial optimization stage, several culture components, including serum, ascorbic acid, and calcium ions, were evaluated for their effects on epithelial differentiation. After 14 days of differentiation, reconstructed tissues were collected for histological analysis to determine the most suitable culture conditions (Fig. 1a). Under optimized conditions, HaCaT cells successfully proliferated and differentiated in the 3D culture system even in the absence of serum. H&E staining revealed a well organized stratified epithelial structure, with columnar basal cells and progressively flattened suprabasal cells, closely resembling the morphology of native human epidermis (Fig. 1b). Although a fully developed stratum corneum was not observed, incomplete keratinization and the absence of a distinct granular layer have also been reported in other reconstructed skin model[13]. The thickness of the reconstructed epithelium ranged from 80 to 200 μm, which is comparable to that reported for commercially available 3D epidermal models.

In native epidermis, basal layer cells retain proliferative capacity. Consistent with this feature, IF staining of the proliferation marker Ki67 demonstrated strong expression in basal layer cells of the reconstructed epithelium, whereas little or no signal was detected in the differentiated suprabasal layers (Fig. 1c). Keratin proteins are key cytoskeletal components of epithelial cells and important markers of epithelial differentiation[14]. In human epidermis, KRT5 and KRT14 are typically expressed in basal keratinocytes, whereas KRT1 and KRT10 are characteristic markers of suprabasal differentiated cells[15]. Accordingly, KRT5 and KRT10 were examined to evaluate the differentiation status of the reconstructed epithelium. IF analysis showed that KRT5 expression was restricted to the basal layer, whereas KRT10 was primarily detected in the suprabasal differentiated layers (Fig. 1d). In addition, E-cadherin, a key mediator of epithelial cell–cell adhesion and tissue integrity[16], was strongly localized along the cell membrane throughout the

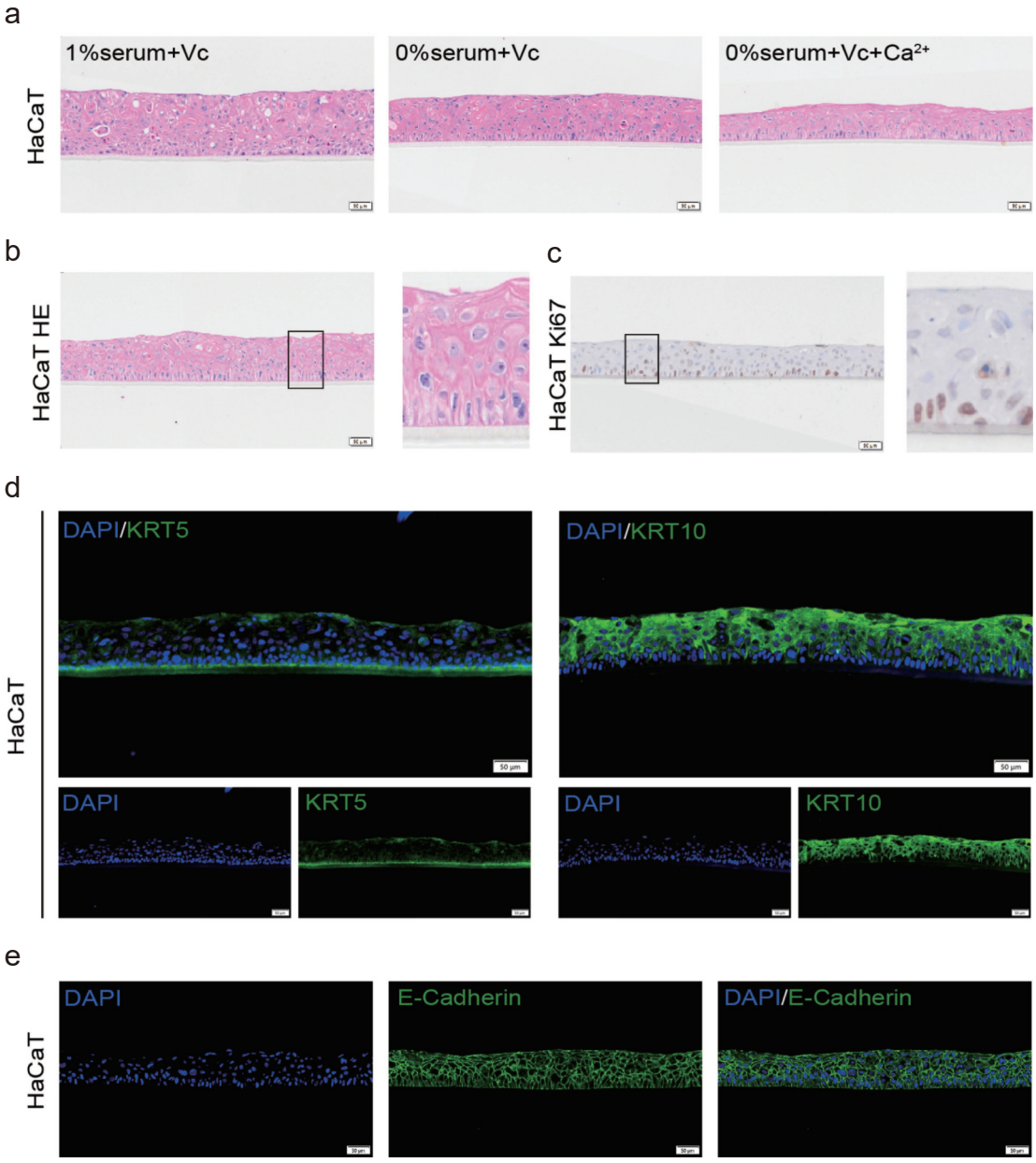

Figure 1 Establishment of a stratified 3D human epidermal model using HaCaT cells. (a) Representative H&E staining of HaCaT derived epithelial constructs under different culture conditions during model optimization. (b) Representative H&E images showing the histological architecture of the differentiated HaCaT epidermal model. Insets indicate local magnified views of epithelial stratification. (c) IHC staining of the proliferation marker Ki67 in the reconstructed epidermal model. (d) IF staining of epithelial differentiation markers KRT5 (basal layer) and KRT10 (suprabasal layers). (e) IF staining of the epithelial adhesion marker E-cadherin. Scale bars: 50 μm.

epithelial layers (Fig. 1e). Together, these findings indicate that the HaCaT-based 3D epithelial model recapitulates key structural and differentiation characteristics of human epidermis.

3.2 Establishment of an oral mucosal epithelial model using HOK cells

Following the successful establishment of a 3D epidermal model using HaCaT cells, we next sought to develop an oral mucosal epithelial model using commonly available oral keratinocyte cell lines. Two cell lines, HOK and NOK, were evaluated for their capacity to generate stratified epithelium under ALI culture conditions. Under serum-free conditions, HOK cells maintained stable proliferative capacity and underwent stratified differentiation in the 3D culture system. In contrast, NOK cells required serum supplementation to sustain proliferation. Because serum is known to interfere with epithelial differentiation, subsequent model optimization focused on HOK cells cultured under serum-free conditions.

During preliminary experiments, we observed pronounced morphological differences in HOK derived epithelial constructs under varying calcium ion concentrations, suggesting that calcium levels play a critical role in epithelial stratification and differentiation. To further investigate this effect, a range of calcium concentrations was tested. The combination of 0.25 mM calcium

ions and ascorbic acid under serum-free conditions was identified as the optimal condition for inducing epithelial stratification (Fig. 2a). Histological analysis revealed a well-organized stratified epithelium with the presence of a keratinized surface layer (Fig. 2b). IF staining of the proliferation marker Ki67 demonstrated strong expression in basal layer cells, while differentiated suprabasal layers showed minimal Ki67 signal, consistent with the proliferative pattern observed in native oral epithelium (Fig. 2c).

In contrast, NOK cells failed to generate a well-differentiated epithelial structure under any tested conditions. Because NOK cells require serum to maintain proliferative capacity in conventional 2D culture, serum supplementation was retained during 3D culture experiments. Although serum supported cell proliferation, it markedly impaired epithelial differentiation. The resulting epithelial

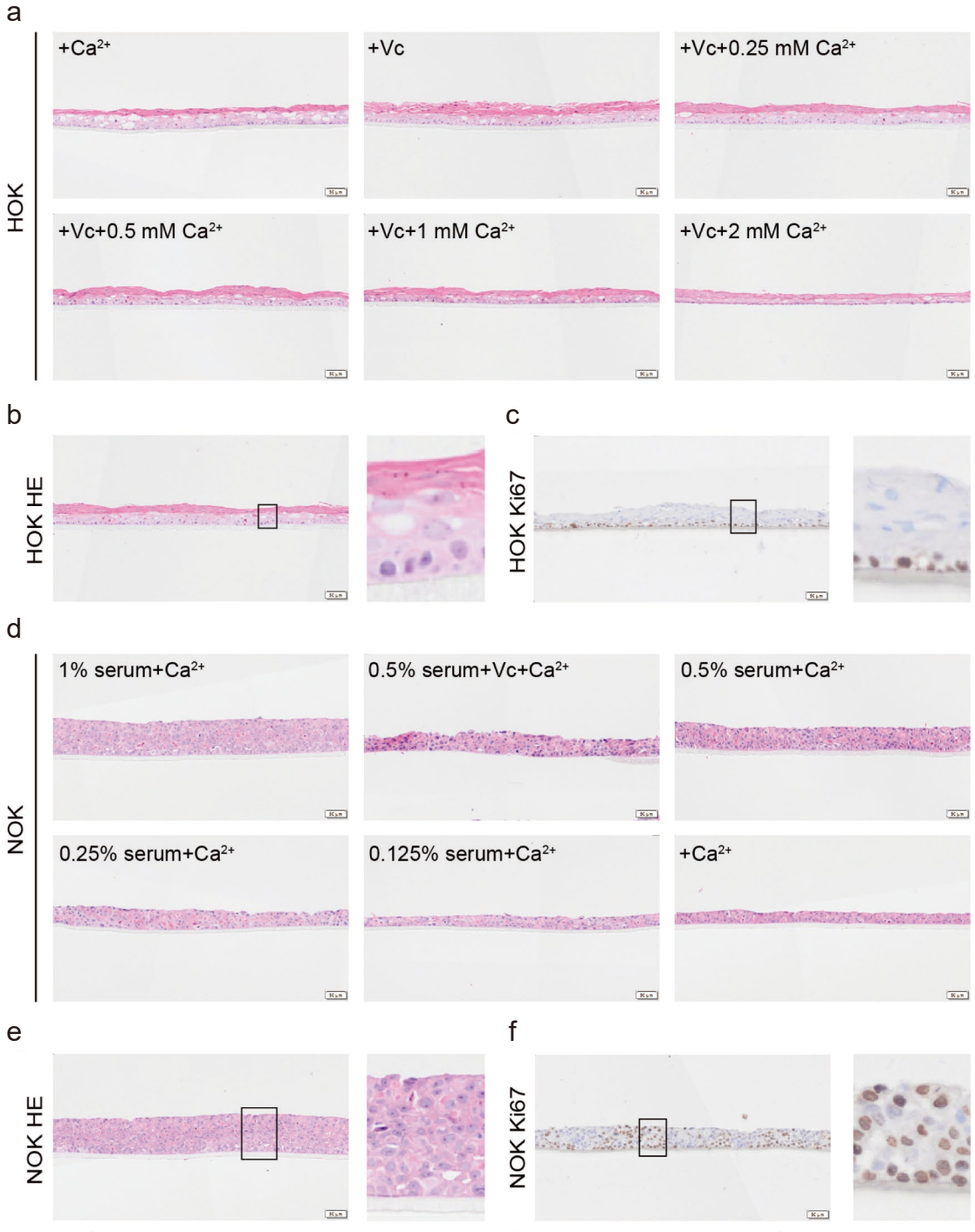

Figure 2 Establishment of an oral mucosal epithelial model using HOK and NOK cells. (a) Representative H&E staining of HOK-derived epithelial constructs under different culture conditions during model optimization. (b) Representative H&E images showing the stratified architecture of the differentiated HOK oral mucosal epithelial model. Insets indicate magnified views of epithelial layers. (c) IHC staining of the proliferation marker Ki67 in the differentiated HOK epithelial model. (d) Representative H&E staining of NOK-derived constructs cultured under different conditions. (e) Higher-magnification H&E images showing the disorganized epithelial structure of NOK-derived constructs. (f) IHC staining of Ki67 in NOK-derived constructs. Scale bars: 50 μm.

constructs displayed disorganized cell layers lacking clear stratification (Fig. 2d, 2e), and Ki67 expression was irregularly distributed across the tissue layers (Fig. 2f). These findings indicate that NOK cells exhibit limited differentiation capacity under the tested conditions, whereas HOK cells are more suitable for constructing stratified oral mucosal epithelial models.

3.3 Oral mucosal epithelial model recapitulates native tissue differentiation characteristics

To evaluate whether the reconstructed oral epithelial model recapitulates native tissue differentiation patterns, several epithelial markers associated with stratification and keratinization were examined. In the oral mucosal epithelium, KRT5 is typically expressed in basal keratinocytes, whereas KRT10 is characteristic of differentiated suprabasal layers. In addition, KRT6 is commonly detected in keratinized oral mucosa such as gingiva and hard palate, where it is associated with epithelial proliferation and mechanical stress responses[17]. Conversely, KRT18 is a marker of simple epithelia and is normally absent in stratified squamous oral mucosa but may appear under pathological conditions[18]. Accordingly, KRT5, KRT10, KRT6, and KRT18 were selected to assess the differentiation fidelity of the reconstructed epithelial models.

IF analysis showed that HOK derived epithelial constructs exhibited a spatial distribution of differentiation markers consistent with native oral mucosa. Although slight morphological differences were observed under varying calcium ion concentrations, the expression patterns of epithelial markers remained consistent. Specifically, KRT5 was localized to the basal layer, KRT10 was detected in suprabasal differentiated layers, and KRT6 was expressed across basal and suprabasal layers but absent from the keratinized surface (Fig. 3a). Importantly, KRT18 was not detected, indicating the absence of abnormal epithelial differentiation. In addition, E-cadherin was strongly localized along the cell membranes throughout the epithelial layers, supporting the

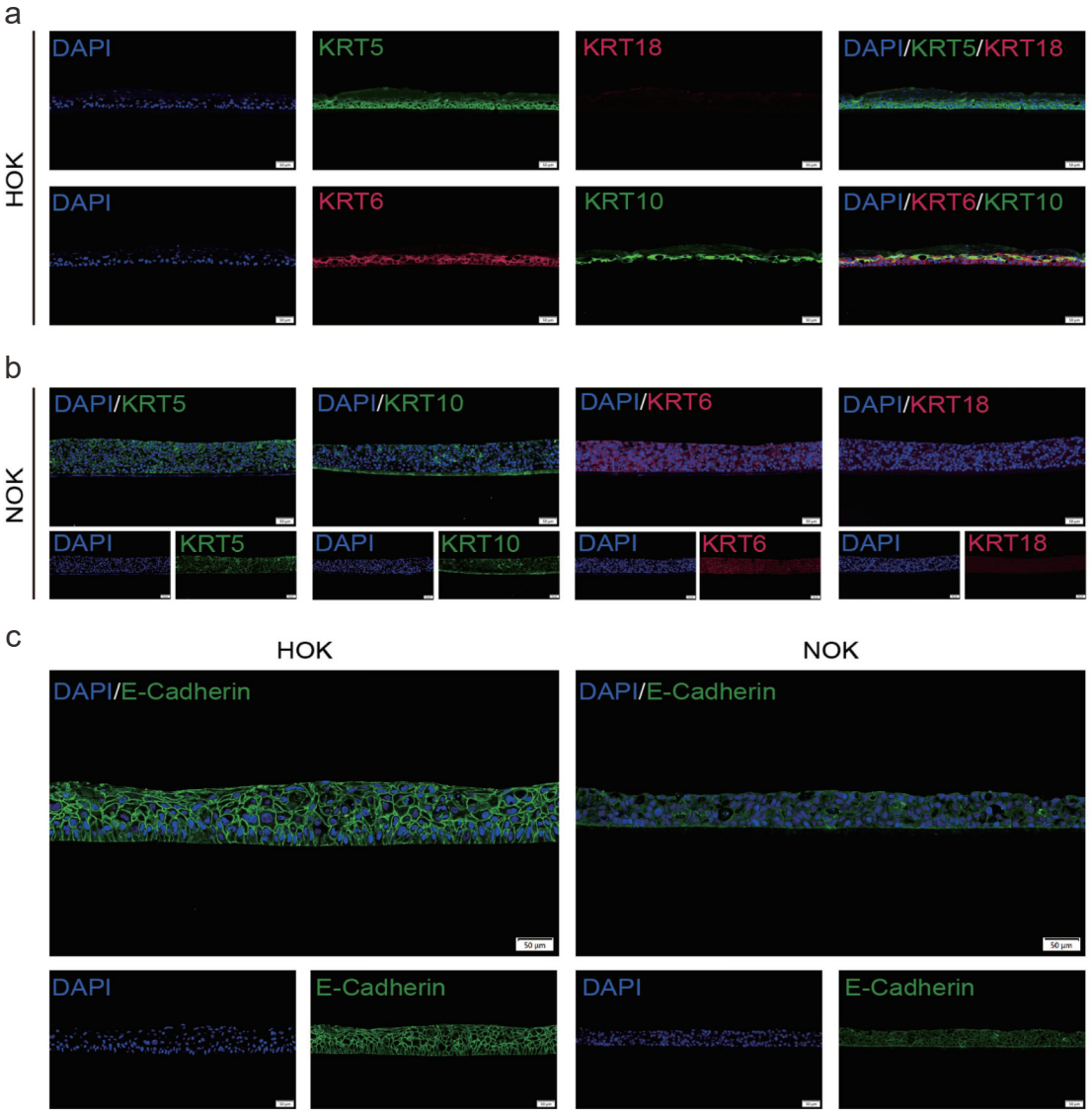

Figure 3 The reconstructed oral mucosal epithelial model recapitulates native tissue differentiation characteristics. (a) IF staining of epithelial differentiation markers KRT5, KRT6, KRT10, and KRT18 in HOK-derived oral mucosal epithelial constructs. (b) IF staining of KRT5, KRT6, KRT10, and KRT18 in NOK-derived constructs. (c) IF staining of the epithelial adhesion marker E-cadherin in HOK- and NOK-derived epithelial constructs. Scale bars: 50 μm.

formation of cohesive epithelial structures (Fig. 3c).

In contrast, NOK derived constructs exhibited disorganized tissue architecture and irregular expression patterns of all tested differentiation markers (Fig. 3b). KRT5, KRT10, and KRT6 displayed diffuse and inconsistent localization, and KRT18 expression was occasionally detected. Furthermore, E-cadherin expression was largely absent (Fig. 3c), indicating impaired epithelial integrity and differentiation. Collectively, these results demonstrate that the HOK derived oral epithelial model closely recapitulates the differentiation characteristics of native oral mucosal epithelium.

3.4 Oral mucosal epithelial model exhibits permeability properties comparable to native epithelium

A key physiological function of stratified epithelial tissues is their selective barrier and permeability capacity. Therefore, the ability to reproduce controlled molecular transport represents an important criterion for validating in vitro epithelial models[19]. To evaluate the permeability properties of the reconstructed epithelia, FITC (MW 389.4 Da) was used as a small molecule tracer. FITC was topically applied to the surface of the epithelial constructs at a non-toxic concentration to mimic physiological exposure to small therapeutic compounds. Due to its hydrophilic nature and well characterized diffusion behavior, FITC is widely used to evaluate passive molecular transport across epithelial barriers[20].

Time-dependent diffusion of FITC within the reconstructed tissues was monitored by fluorescence imaging along the vertical axis of the epithelial constructs. In the HaCaT based epidermal model, FITC was largely confined to the superficial layer at 12 h, penetrated to the middle layers by 24 h, and reached the basal layer by 48 h, with fluorescence intensity gradually increasing over time (Fig. 4a). In the HOK derived oral mucosal model, FITC exhibited a similar diffusion pattern but with slightly faster initial penetration. At 12 h, FITC had already reached the middle epithelial layers, and by 48 h the fluorescence signal extended to approximately 65% of the total epithelial thickness (Fig. 4b). Despite these differences in early diffusion kinetics, the overall distribution profiles of FITC in both models were comparable at later time points. Semi-quantitative analysis further confirmed a time dependent increase in cumulative permeability in both HaCaT and HOK epithelial models (Fig. 4c, 4d). Together, these results indicate that the reconstructed epithelial models exhibit dynamic permeability characteristics consistent with native epithelial tissues, supporting their suitability for studies of epithelial barrier function and drug transport.

3.5 Application of the model in host pathogen interaction studies

To evaluate the applicability of the reconstructed epithelial models for infection studies, a co-culture system with *C. albicans* was established to simulate host pathogen interactions in vitro[21]. Infection assays were performed by inoculating *C. albicans* onto the surface of the 3D epithelial constructs, and samples were collected at 12, 24, and 48 h post infection. PAS staining revealed progressive fungal invasion over time. At 12 h, *C. albicans* exhibited early hyphal germination, with short hyphae adhering to the epithelial surface. By 24 h, hyphal structures had expanded and penetrated into the suprabasal epithelial layers, forming localized invasive foci. At 48 h, extensive hyphal invasion was observed beneath the basal layer, accompanied by basal cell damage and marked disruption of epithelial architecture (Fig. 5). Notably, the oral mucosal model derived from HOK cells exhibited more rapid and deeper fungal penetration compared with the HaCaT based epidermal model. These observations suggest that intrinsic differences in tissue specific barrier properties influence the efficiency and progression of fungal invasion. Together, these results demonstrate that the reconstructed epithelial models can effectively support host pathogen interaction studies and provide a useful in vitro platform for investigating epithelial colonization and invasion by *C. albicans*.

4 Discussion

In this study, we developed a phase regulated culture system consisting of three functionally complementary media modules, in which distinct medium compositions were applied at different stages of epithelial culture. This modular design maintains relative compositional simplicity while supporting both keratinocyte proliferation and differentiation. During two-dimensional expansion, the culture conditions provide sufficient nutrients while preserving the differentiation potential of keratinocytes. Following transition to three-dimensional culture, the optimized conditions enable orderly epithelial stratification and differentiation (Fig. 1b and Fig. 2b). Importantly, the use of widely available keratinocyte cell lines eliminates the need for repeated isolation of primary cells, thereby improving experimental reproducibility and scalability. Such cell line based reconstruction strategies have been increasingly explored as practical alternatives to primary cell dependent epithelial models.

HaCaT keratinocytes are spontaneously immortalized cells that retain the capacity to undergo epidermal differentiation and recapitulate stratified epithelial architecture in vitro. Based on this epidermal model (Fig. 1), we further established a practical oral mucosal epithelial model using HOK cells, which are commonly employed in oral and dental research. The reconstructed oral epithelium exhibited a stratification pattern, proliferation distribution, and degree of keratinization comparable to native oral mucosa (Fig. 2b and Fig. 3a). Interestingly, the relative thickness of the suprabasal and keratinized layers appeared similar in the reconstructed tissue, which may indicate subtle imbalances between basal proliferation and terminal differentiation during in vitro epithelial reconstruction. In contrast, NOK cells failed to generate a well-differentiated epithelial structure under the tested conditions (Fig. 2d-2f and Fig. 3b). A likely explanation lies in the distinct culture requirements of this cell line. Unlike HaCaT and HOK cells, which successfully stratified under serum-free conditions, NOK cells required serum supplementation to sustain proliferation. However, serum supplementation interfered with epithelial differentiation, preventing the formation of a stable stratified epithelium. Future work will focus on identifying serum-free culture conditions capable of supporting both proliferation and differentiation of NOK cells in order to further expand the applicability of the model.

Functional validation demonstrated that both reconstructed epithelial models exhibit permeability properties consistent with native epithelial tissues. The HOK derived oral mucosal model displayed faster initial diffusion kinetics of FITC compared with the HaCaT based epidermal model (Fig. 4), which likely reflects intrinsic physiological differences between oral mucosa and skin epidermis. The skin epidermis forms a highly effective barrier

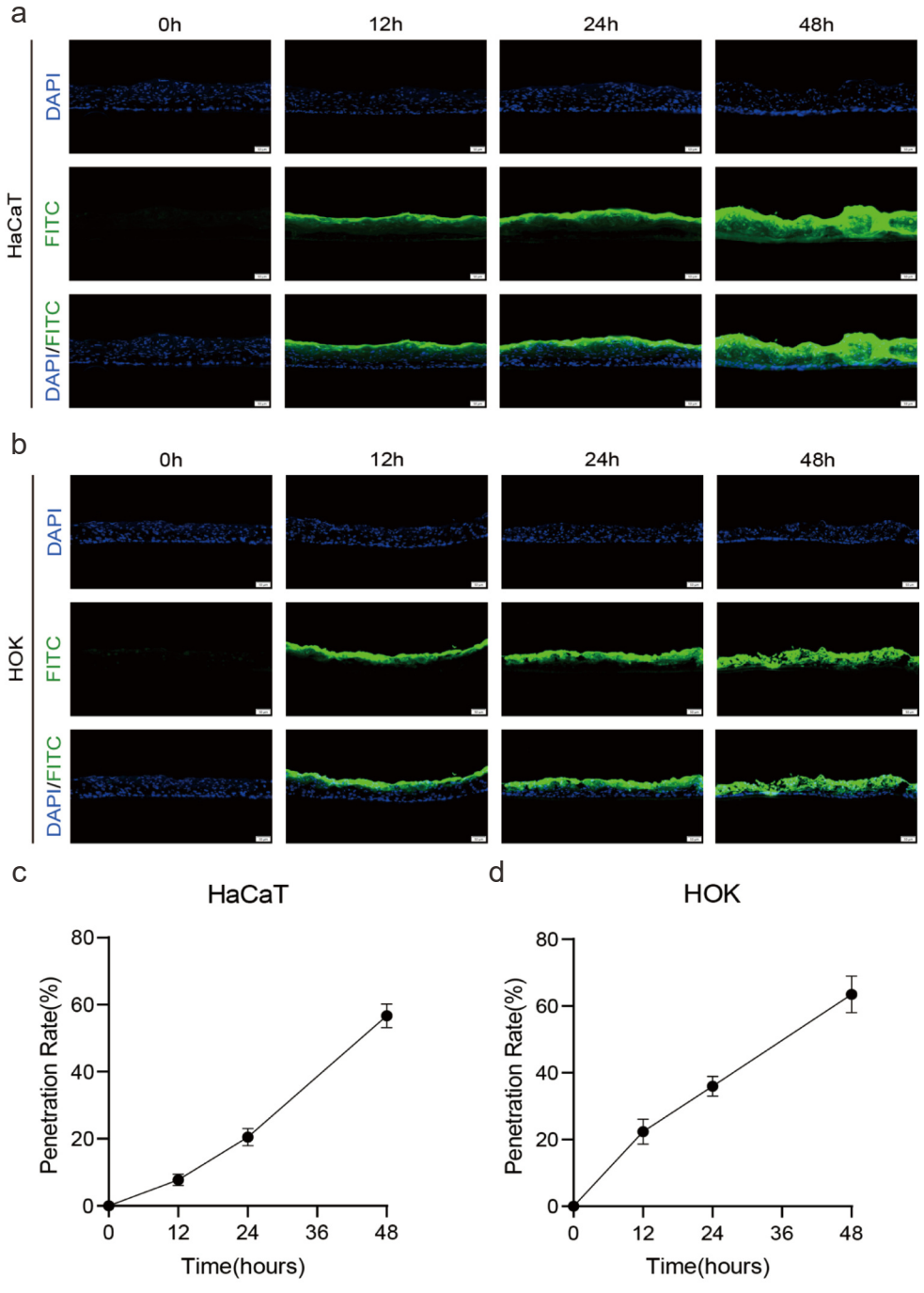

Figure 4 Permeability properties of reconstructed epithelial models. (a) Representative fluorescence images showing time-dependent diffusion of FITC in the HaCaT-derived epidermal model at 0, 12, 24, and 48 h. (b) Representative fluorescence images showing time-dependent diffusion of FITC in the HOK-derived oral mucosal epithelial model at 0, 12, 24, and 48 h. (c) Semi-quantitative analysis of FITC permeability in the HaCaT epidermal model at different time points (n = 3). (d) Semi-quantitative analysis of FITC permeability in the HOK oral mucosal epithelial model at different time points (n = 3). Scale bars: 50 μm.

through dense keratinization and lipid rich lamellar structures, whereas oral mucosa generally exhibits reduced keratinization and increased permeability to hydrophilic molecules. These structural differences are consistent with the clinically observed rapid absorption of certain drugs administered through the oral mucosa.

We further assessed the suitability of the reconstructed epithelial models for host pathogen interaction studies using *Candida albicans*. The transition of *C. albicans* from yeast to hyphal morphology and subsequent epithelial penetration represent critical steps in mucosal infection and barrier disruption[22]. In our co-culture system, the oral epithelial model showed more rapid and deeper hyphal invasion compared with the epidermal model (Fig. 5), reflecting the known susceptibility of oral mucosa to fungal colonization. This difference may arise from structural and microenvironmental factors, including reduced keratinization,

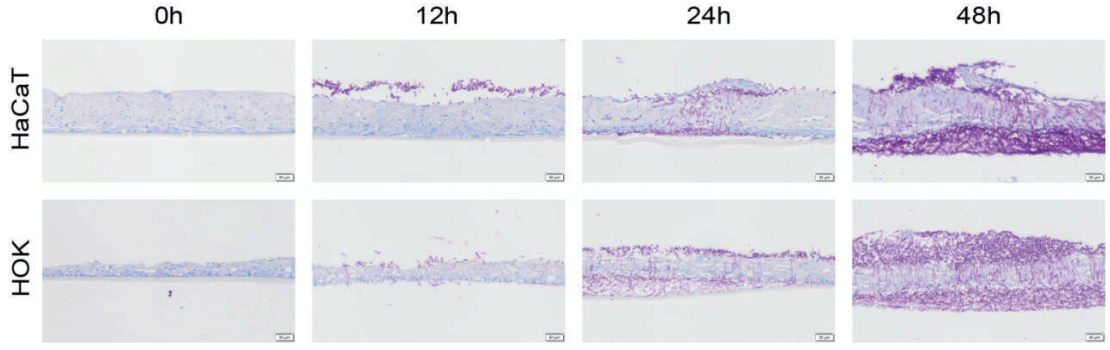

Figure 5 Application of reconstructed epithelial models in host–pathogen interaction studies. Representative PAS staining images showing time-dependent invasion of *C. albicans* in the HaCaT-derived epidermal model and the HOK-derived oral mucosal epithelial model at 0, 12, 24, and 48 h post-infection. Scale bars: 50 μm.

neutral pH conditions, and saliva associated components that facilitate fungal adhesion and invasion, whereas the skin epidermis provides stronger physical and immunological barriers[23]. These results suggest that the model captures tissue-specific differences in epithelial susceptibility and may therefore provide a useful platform for studying fungal infection mechanisms and evaluating antifungal therapeutic strategies.

Overall, the reconstructed epithelial models presented in this study address several limitations of conventional in vitro systems by combining structural fidelity, experimental accessibility, and reproducibility. The platform provides a versatile tool for investigating epithelial biology, studying mechanisms of skin and oral diseases, and evaluating drug transport or antimicrobial interventions in physiologically relevant tissue environments.

Acknowledgments

The authors gratefully acknowledge support from the National Natural Science Foundation of China (NSFC) (Grant Nos. 82470984, 82271035, U25A6003, 82330029, 32200577), National Key Research and Development Program of China (Grant Nos. 2022YFC2402901), for financial support.

Data available statement

All data supporting the findings of this study are available within the article or from the corresponding author upon reasonable request.

Author contribution

L.L., L.J., Y.Y. and Z.H. contributed conception and design of the study. L.L. contributed to experiments and writing-original draft. L.J., Y.Y. and Z.H. contributed to writing-review & editing. Y.Y. and Z.H. supervised the work and contributed to the funding acquisition. All authors have read and approved the final manuscript.

Ethics approval and consent

N/A

Consent for publication

All authors have reviewed and approved the manuscript for publication.

Conflicts of interest

The authors declared no potential conflicts of interest concerning the research, authorship, and/or publication of this article.

References

[1] Harris-Tryon, T. A.; Grice, E. A. Microbiota and maintenance of skin barrier function. *Science* **2022**, *376*, 940–945.
[2] Williams, D. W.; Greenwell-Wild, T.; Brenchley, L.; et al. Human oral mucosa cell atlas reveals a stromal-neutrophil axis regulating tissue immunity. *Cell* **2021**, *184*, 4090–4104.e15.
[3] A.L. Haber; M. Biton; N. Rogel; et al. A single-cell survey of the small intestinal epithelium. *Nature* **2017**, *551*, 333–339.
[4] Mazzinelli, E.; Favuzzi, I.; Arcovito, A.; et al. Oral mucosa models to evaluate drug permeability. *Pharmaceutics* **2023**, *15*, 1559.
[5] Bissell, M. J.; Radisky, D. Putting tumours in context. *Nat. Rev. Cancer* **2001**, *1*, 46–54.
[6] Moharamzadeh, K.; Brook, I. M.; Van Noort, R.; et al. Tissue-engineered oral mucosa: A review of the scientific literature. *J. Dent. Res.* **2007**, *86*, 115–124.
[7] Klausner, M.; Handa, Y.; Aizawa, S. *In vitro* three-dimensional organotypic culture models of the oral mucosa. *Vitro Cell. Dev. Biol. Anim.* **2021**, *57*, 148–159.
[8] Buskermolen, J. K.; Reijnders, C. M. A.; Spiekstra, S. W.; et al. Development of a full-thickness human gingiva equivalent constructed from immortalized keratinocytes and fibroblasts. *Tissue Eng. Part C Meth.* **2016**, *22*, 781–791.
[9] Yuan, Y.; Park, J.; Feng, A.; et al. YAP1/TAZ-TEAD transcriptional networks maintain skin homeostasis by regulating cell proliferation and limiting KLF4 activity. *Nat. Commun.* **2020**, *11*, 1472.
[10] Kehe, K.; Abend, M.; Kehe, K.; et al. Tissue engineering with HaCaT cells and a fibroblast cell line. *Arch. Dermatol. Res.* **1999**, *291*, 600–605.
[11] Dongari-Bagtzoglou, A.; Kashleva, H. Development of a highly reproducible three-dimensional organotypic model of the oral mucosa. *Nat. Protoc.* **2006**, *1*, 2012–2018.
[12] Mansour, F.; Parisi, L.; Rihs, S.; et al. Immortalization of patient-derived lip cells for establishing 3D lip models. *Front. Cell Dev. Biol.* **2024**, *12*, 1449224.
[13] Itoh, M.; Umegaki-Arao, N.; Guo, Z. Y.; et al. Generation of 3D skin equivalents fully reconstituted from human induced pluripotent stem cells (iPSCs). *PLoS One* **2013**, *8*, e77673.
[14] Shetty, S.; Gokul, S. Keratinization and its disorders. *Oman Med. J.* **2012**, *27*, 348–357.
[15] Presland, R. B.; Dale, B. A. Epithelial structural proteins of the skin and oral cavity: Function in health and disease. *Crit. Rev. Oral Biol. Med.* **2000**, *11*, 383–408.

[16] Tunggal, J. A.; Helfrich, I.; Schmitz, A.; et al. E-cadherin is essential for *in vivo* epidermal barrier function by regulating tight junctions. *EMBO J.* **2005**, *24*, 1146–1156.
[17] Chu, P. G.; Weiss, L. M. Keratin expression in human tissues and neoplasms. *Histopathology* **2002**, *40*, 403–439.
[18] Yan, J. Z.; Yang, A. W.; Tu, S. The relationship between keratin 18 and epithelial-derived tumors: As a diagnostic marker, prognostic marker, and its role in tumorigenesis. *Front. Oncol.* **2024**, *14*, 1445978.
[19] Bierbaumer, L.; Schwarze, U. Y.; Gruber, R.; et al. Cell culture models of oral mucosal barriers: A review with a focus on applications, culture conditions and barrier properties. *Tissue Barriers* **2018**, *6*, 1479568.
[20] Hoogstraate, A. J.; Cullander, C.; Nagelkerke, J. F.; et al. Diffusion rates and transport pathways of fluorescein isothiocyanate (FITC)-labeled model compounds through buccal epithelium. *Pharm. Res.* **1994**, *11*, 83–89.
[21] Yadev, N. P.; Murdoch, C.; Saville, S. P.; et al. Evaluation of tissue engineered models of the oral mucosa to investigate oral candidiasis. *Microb. Pathog.* **2011**, *50*, 278–285.
[22] Tabatabaei, F.; Moharamzadeh, K.; Tayebi, L. Three-DimensionalIn VitroOral mucosa models of fungal and bacterial infections. *Tissue Eng. Part B Rev.* **2020**, *26*, 443–460.
[23] Gaffen, S. L.; Moutsopoulos, N. M. Regulation of host-microbe interactions at oral mucosal barriers by type 17 immunity. *Sci. Immunol.* **2020**, *5*, eaau4594.